

Experimental and numerical investigation of reinforced concrete beams containing vertical openings

Jafarali Parol^{1*}, Ammar Ben-Nakhi^{2a}, Shaikha Al-Sanad^{1b}, Jamal Al-Qazweeni^{1c},
Hamad J. Al-Duaij^{1d} and Hasan Kamal^{1e}

¹Kuwait Institute for Scientific Research, Kuwait

²Kuwait University, Kuwait

(Received December 24, 2018, Revised June 15, 2019, Accepted June 20, 2019)

Abstract. Horizontal openings in reinforced concrete (RC) beams are quite often used to accommodate service pipelines. Several research papers are available in the literature describing their effect. RC beams with vertical openings are commonly used to accommodate service lines in residential buildings in Kuwait. However, there are lack of design guidelines and best practices reported in the literature for RC beams with vertical openings, whereas the detailed guidelines are available for beams with horizontal openings. In the present paper, laboratory experiments are conducted on nine RC beams with and without vertical openings. Parametric study has been carried out using nonlinear finite element analysis (FEA) with changes in the diameter of the opening, various positions of the opening along the length and width of the beam, edge distance, etc. 50 finite element simulations were conducted. The FEA results are verified using the results from the laboratory experiments. The study showed that the load carrying capacity of the beam is reduced by 20% for the RC beam with vertical openings placed near the center of the beam compared to a solid beam without an opening. Significant reduction in load carrying capacity is observed for beams with an opening near the support ($\approx 15\%$). The overall stiffness of the beam, crack pattern and failure modes were not affected due to the presence of the vertical opening. Furthermore, an artificial neural network (ANN) analysis is carried out using the FEA generated data. The results and observations from the ANN and FEA are in good agreement with experimental results.

Keywords: reinforced concrete beam, vertical opening, finite element analysis, artificial neural network

1. Introduction

Transverse openings (Fig. 1) in reinforced concrete (RC) beams are commonly used in practice to accommodate services such as electricity, water supply, internet network, etc. Transverse opening in RC beams can be of different shapes and sizes. Circular and rectangular openings are of most practical interests as they are most commonly used. It is quite well known that the stress concentration occurs around the openings (Savin (1951), Heller (1953)). These conclusions are not directly applicable in RC beams, due to nonlinear post-cracking behavior. Beams with openings need special treatment in analysis and design as they cause a disturbance in the load distribution around the opening.

Openings cause the internal forces (bending moment and shear force) redistribution and load path change within the structural member. This is especially true if the opening is large. The surrounding area of the opening is a D-region, where the linear strain distribution based on Euler Bernoulli's beam theory is not applicable. In general, analysis procedure and design criterion of beams with openings are different from that of a solid beam. Beams with openings could be carefully designed to achieve the desired serviceability and strength requirements. Lorensten (1962) was the first to explain the shear force distribution around the opening. According to him, the total shear around the opening is carried by the compression chord, and the tension chord does not share any applied shear. This argument probably valid only partially, because, if the openings were near the compression side, then the tension chord will also share a portion of the applied shear force. Nasser *et al.* (1967) offered a simple linear theory of applied shear force distribution near the opening based on the area of cross-section of the bottom and top chord. Size of the opening is one of the critical parameters that determine the structural behavior of beams with openings. Laboratory experimental results indicate that a beam with small openings under-reinforced in shear fails in the same mode as that of a solid beam (Hanson, 1969). Somes and Corely (1974) reported that the vertical location of the opening has no significant effect on the load carrying capacity of the RC beam. On the other hand, Kong and

*Corresponding author, Ph.D.

E-mail: jparol@kisir.edu.kw

^a Associate Professor

E-mail: ammarnakhi@yahoo.com

^b Associate Research Scientist

E-mail: ssanad@kisir.edu.kw

^c Associate Research Scientist

E-mail: jqazweeni@kisir.edu.kw

^d Associate Research Scientist

E-mail: hduaij@kisir.edu.kw

^e Research Scientist

E-mail: hkamal@kisir.edu.kw



Fig. 1 RC beams with different types of openings

Sharp (1977) observed that location and size of the opening affect the shear strength of a deep beam containing an opening. Kong *et al.* (1978) derived an empirical formula for estimating the shear strength of deep beams.

Mansur and co-workers conducted pioneering and original research on RC beams with openings and proposed design procedure for beams with openings (Mansur *et al.* (1982), Mansur (1983), Mansur *et al.* (1983a, & 1983b), Mansur *et al.* (1984), Mansur *et al.* (1985), Mansur (1988), Mansur *et al.* (1991a & 1991b)). In their study, the effect of number of spans, size, and x-location of openings was examined. Mansur *et al.* (1991a & 1991b) observed early cracking, reduction in the strength and stiffness of the beam with an increase of the size of openings. Openings located in a high moment region resulted in the early collapse of the beam. They idealized load-deflection curve of an RC beam containing a large opening by a piecewise linear approximation. In this method, the hinge formation is traced by successive elastic analyses. Total deflections were calculated by linear superposition of deflections caused by flexural action on the entire beam to those produced by shear at the opening. In their analysis, chord members were treated as double cantilevers. The method was verified with available test data on a simply supported, a two-span continuous, and five three-span continuous beams. Tan *et al.* (1996) conducted an experimental study on 15 RC T-beams with large web openings. They observed that the applied shear force is distributed among the chords in the same ratio of their flexure stiffness based on either gross or cracked transformed section. They reported that the presence of web openings leads to a decrease in ultimate strength and post-cracking stiffness. Their study confirmed Vierendeel panel behavior at the openings of the beam. Mansur (1998) observed two independent cracking patterns separating the beam into two different segments above and below the opening. Such independent crack and the resulting failure patterns were termed as “frame type” failure. In the “Beam type” failure, the failure plane passes through the center of the opening (Fig. 2). He suggested different design procedure for these two types of failure modes.

In the 1980's, circular and square openings in RC beams were considered as small openings by several authors (Hasnat and Akhtaruzzaman (1987)). Mansur and Tan (1999) later recommended a better criterion that can be used to classify the size of an opening as either large or small based on the dimension and location of the opening, and size of the beam. Their classification was initially developed based on studies of rectangular openings. They also offered the formula to be used for classification of circular openings. Circular openings less than 40%

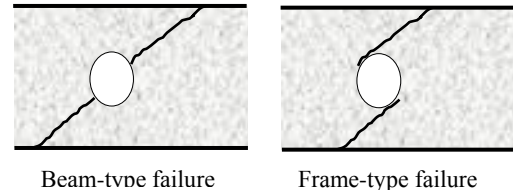


Fig. 2 Possible crack patterns in RC beams with openings

(approximately) of the overall depth of the beam is considered as a small opening. They provided guidelines for the design of RC beams with openings. As a thumb rule, they suggested that the depth of openings shall not exceed half of the total depth of the beam, and the opening should not be located near supports. According to them, if the opening size and locations were carefully chosen, the load transferring mechanism and load carrying capacity might not alter much compared to a similar solid beam. Analysis and design of post-tensioned concrete beams with rectangular openings were presented by Kennedy and Abdalla (1992).

Aykac *et al.* (2013) conducted an experimental study to examine the effect on the flexural behavior of an RC beam containing multiple openings along the length. According to them, the length of the plastic hinges increased for beams containing multiple openings compared to beams with a single opening. They observed that special reinforcement around the opening such as diagonal reinforcement, longitudinal rebars and full-depth stirrups adjacent to openings and short stirrups in the chords effectively prevented premature failure of the beam. Recently, Samar *et al.* (2017) examined the flexural performance of a self-compacted perforated beam system using the experimental method.

Various analytical methods have been employed to predict the load carrying capacity of an RC beam containing an opening. Strut and tie model was proposed for the analysis of deep beams containing opening by several authors (Hwang *et al.* (2000), Tan *et al.* (2003), Chien-Chuang *et al.* (2017)). The strut and tie methods, in general can be applied for deep beams with or without openings. Beams with horizontal openings have been examined experimentally and numerically by several investigators and the load transfer mechanism is well established. Hence the application of strut and tie method in the case of beams with horizontal openings is relatively straight forward. On the other hand there was no experimental work or numerical simulation work was reported in the literature for beams with vertical openings and the load transfer mechanism is little known in this case. Therefore, the application of strut and tie method may not be straight forward in this case. Moreover, for beams with vertical opening, if the opening is not placed in the middle of the beam along the width, then the strut and tie method may not be applicable in the current form. This is a possible area of research for the application of the strut and tie method.

Nonlinear finite element analysis has been used for the analysis of RC beams containing opening under flexural

load by several investigators (Al-Shaarbaf *et al.* (2007), Doh *et al.* (2012), Lisantono (2013), Osman *et al.* (2017), Karimi and Hashemi (2018)). A state-of-the-art literature review was published by Ahmed *et al.* (2012) on RC beams containing openings.

In general, the opening is a potential weak area in an RC beam and demands post-cracking strengthening probably by FRP or by other means. Strengthening the RC beam by FRP was investigated in (El-Maaddawy and Al-Ariss (2012), Lu *et al.* (2012), Hawileh *et al.* (2012), Lu *et al.* (2014), Chin *et al.* (2015), Chin *et al.* (2016), Behfarnia and Shirneshan (2017), Nie *et al.* (2018)).

Reinforced concrete framed structural systems are commonly employed in the residential buildings of Kuwait. Plumbing and other service pipes are passed through vertical openings in the RC beams. The location of the vertical pipe passed through an RC beam in a typical residential building in Kuwait is depicted in Fig. 3. The vertical openings are incorporated only during the construction stage and are not considered during the structural design stage. As a result, the vertical openings are provided, probably ignoring its effect on the beam capacity. The pipes are installed during the formwork stage of the construction. Typically these openings are created in the beam adjacent to the column joint.

In the present paper, experimental and detailed numerical study has been conducted to examine the effect of vertical openings on the RC beams. Laboratory experiments have been conducted on nine beams. The effect of the size of the opening, location of the opening along the length and width of the beam has been examined. Nonlinear finite element analysis has been conducted with various parameters on 50 RC beam models with and without opening. The finite element models are benchmarked against the laboratory experimental results. It is observed that location and size of the vertical opening has a significant effect RC beams. 20% reduction in the ultimate strength is observed for beams containing vertical opening at the mid-span region. As the size of the opening increases, a sharp reduction in ultimate strength is observed, especially when the edge distance from the circumference of the opening reduces to less than a certain value. In this study, this limiting value is attributed to the minimum cover distance.

2. Research significance

Openings (vertical or horizontal) in RC beam can cause reduction in load carrying capacity, influence the failure mode, ductility behavior, stiffness of the beam etc. Though extensive studies have been carried out on RC beam with horizontal openings, there is a lack of research on RC beams with vertical openings. There are clear guidelines available for horizontal openings in RC beams. However, there are no guidelines or design practices available for vertical openings in RC beams. RC beams with vertical openings are often used in practice without following any standard design guidelines. It is a quite common practice to use vertical openings in RC beams for service lines of residential buildings in Kuwait (Fig 3). Transverse opening



Fig. 3 Service pipes installed through vertical openings in the RC beams in a typical residential building in Kuwait

(horizontal) will affect the flexural and shear strength of the beams based on the size, shape, and location of the openings and loading conditions of the beam. It is not clear that the same conclusions can be extended to the vertical openings in the beam. In this paper, structural behavior of RC beams with vertical openings is examined. This study intends to gain more fundamental understandings of the effect of size, and locations of vertical openings in RC beams that could enhance knowledge and design practices of RC beams with vertical openings to improve the load carrying capacity, durability etc. Outcome of this study will help developing a local design guideline for practicing engineers to incorporate the effect of vertical openings during the design stage.

3. Research program

The research program includes three parts. In the first part, an experimental investigation is conducted with three different test beams. Two beam specimens containing openings and one beam without opening have been examined. Beams without opening are considered as a reference beam. Three tests were conducted on each case with a total of nine laboratory experiments. In the second part, a nonlinear Finite Element (FE) model is benchmarked using laboratory results. Extensive parametric study is then performed using the FE model. In the third part of the study, an ANN analysis is employed to verify the FEA results and laboratory experiments.

3.1 Experimental testing program

3.1.1 Test specimen

The main objective of the experimental program was to examine the load carrying capacity, failure mode and the crack pattern of a fixed-fixed reinforced concrete beam under flexural load. In the laboratory experiment, the fixed-fixed boundary condition is used to simulate the actual condition that is being employed in a framed structure used for a typical residential building in Kuwait. Three different geometrical configurations were examined as given below:

Case 1: RC beam without opening (used as reference beam).

Case 2: RC beam containing a vertical opening throughout the depth of the beam. The diameter of the

Table 1 Geometric details of the beam specimen used for the laboratory experiment

Case	Geometric details			Opening details			Ratio (2x/L)
	Effective span (L) (mm)	Width (b) (mm)	Depth (h) (mm)	Main reinforcement	Diameter (d) (mm)	Distance of center of opening from left support (x) (mm)	
Beam without opening	2200	200	400	2 ϕ 16	-	-	-
Opening near left support	2200	200	400	2 ϕ 16	110	220	0.5
Opening at the center of the beam	2200	200	400	2 ϕ 16	110	1100	1

opening is 110 mm, and it is located at 220 mm from the left end of the support.

Case 3: Similar to case 2, but the location of the opening is at the center of the beam.

Test specimen descriptions are presented in Table 1 and Fig. 4. The total length of the beam is 2200 mm. Both ends of the beam were clamped using steel plates to ensure the fixed support condition of the beam. The beam is reinforced with 2 ϕ 16 bars at the bottom and top of the beam and ϕ 10 shear stirrups are placed 120 mm uniform spacing along the length of the beam. The ratio of the diameter of the opening to the depth of the beam is 0.275. It is worth noting that, there are no descriptions available in the literature, to classify the vertical opening either as large or small. In the present paper, the opening is called merely as “opening” without the terms “small” or “large”.

3.1.2 Material characteristics and specimen preparation

Ready-mixed concrete, typically used in the construction of residential buildings in Kuwait was used in the present study. Mix proportion of the ready-mix concrete is presented in Table 2. Nine wooden formworks are used to cast the samples. The reinforcement cage is placed in the wooden formwork, and the pipe is placed through the reinforcement cage to create a vertical opening in the beam as shown in Fig. 5. Concrete is cast and cured for 28 days, and formwork was removed. Three samples from each case were tested. The average compressive and tensile strengths of the concrete were 39.6 MPa and 3.4 MPa respectively.

3.1.3 Experimental setup

Formwork and structural loading arrangements are presented in Figs. 5 & 6 respectively. The test beam was fixed at both ends using a high strength steel plate (200 mm x 500 mm x 100mm) and steel bolts to ensure the fixity without rotation or yielding of the support. The plate was connected at the end of the beam with four bolts of 35 mm

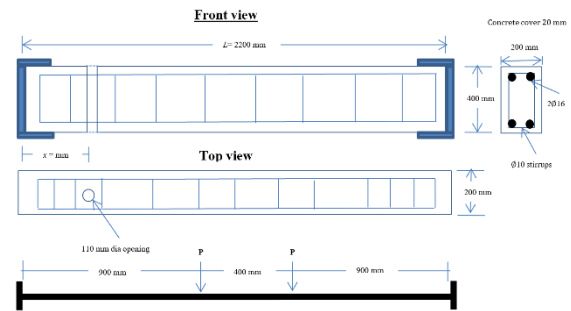


Fig. 4 Geometrical details of a typical test sample used in the experiment

Table 2 Mix proportion of ready mixed concrete (kg/m³)

Constituent Concrete	Weight (kg/ m ³)
Cement	350
Water-cement ratio	0.57
Sand	750
Aggregate (18 mm)	500
Aggregate (13 mm)	300
Aggregate (9 mm)	250
Superplasticizer	2.75
Total weight of the mix	2350

diameter. The yield strength of the material of the steel plate was 405 MPa, and that of the steel bolt was 665 MPa. The beams were subjected to four-point loading, and the actuator load was transferred to the beam using a spreader beam supported on two steel rods (Fig. 6). The two steel rods were spaced at 400 mm. All test specimens were tested until failure. The load was applied at a speed of 0.15 kN /sec. Midspan deflection of the beam was recorded using a deflection dial gauge placed at the bottom of the beam. Crack initiation and crack propagation were marked, and the failure mode was recorded.

4. Experimental results

4.1 Beam without opening (Reference beam)

Load-displacement curve and the crack pattern obtained from the structural load test for the reference test specimen without opening is depicted in Figs. 7 & 8 respectively. The failure load and maximum displacement are presented in Table 3. Average stiffness of the beam in the linear portion of the load displacement curve is 30.63 kN/mm. The first crack appeared at the soffit of the beam in nearly in the vertical position. Subsequently, several flexural cracks appeared near the mid-span, and these cracks widened and propagated with increase of applied load. Simultaneously, several cracks appeared from the topside of the fixed end supports of the beam. The beam specimens failed at an average load of 282.5 kN. Maximum recorded displacement at mid-span of the beam was 20 mm. The beam failed with a typical flexure failure mode at the mid-span of with vertical crack from the soffit of the beam and also concrete crushing from the top mid span location (Fig. 8a).



Fig. 5 Formwork of beams samples and installed vertical pipe for the experiment



Fig. 6 The structural testing test set up for the beam

4.2 Beam with an opening at 220 mm from the support

For this case beam opening was placed at the 220 mm from the left support. Average stiffness of the beam in the linear portion of the load displacement curve is 30.57 kN/mm. It is interesting to note that there was not reduction in the overall stiffness of the beam due to the vertical opening as indicated by the slope of the load-displacement curve. The beam failed at an average load of 277.3 kN with a 2% reduction in the load carrying capacity compared to the baseline case without an opening, which is quite an insignificant reduction. The load-displacement curve for this case is shown in Fig. 7. The maximum vertical deformation at the mid-span before failure was 17 mm. There were multiple surface cracks generated from the periphery of the opening towards the edge of the beam. These cracks did not develop full depth of the beam. The overall crack pattern at failure load was similar to the beam without opening (Fig. 8b).

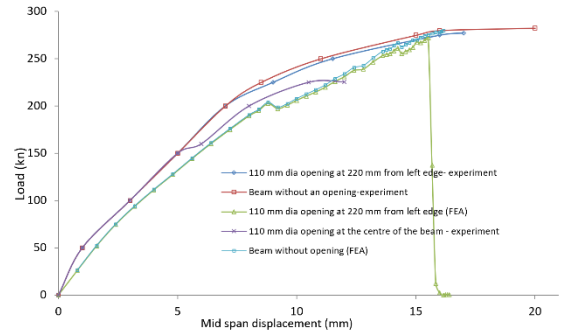


Fig. 7 Load-displacement curve for the experiments and FEA

Table 3 Failure load and maximum displacement from laboratory experiments

Specimen Description	Laboratory experiment		% Reduction in failure load
	Failure Load (kN)	Max Deflection (mm)	
Reference beam without opening	282.5	20	
110 mm dia opening @ 220 mm from the left support	277.3	17	1.8
110 mm dia opening @ mid span	225.3	12	19

4.3 Beam with an opening at mid-span of the beam

The beam with an opening in the mid-span of the beam failed at an average load of 225.3 kN with a reduction of approximately 20% compared to the beam without an opening. Maximum deflection before failure was 12 mm, and a significant reduction in load carrying capacity was observed compared to the reference beam. It is interesting to note that the slope of the load-displacement curve for three test cases were almost the same. In other words, the presence of the opening irrespective of the location did not alter the overall stiffness of the beams. It is worth mentioning that, this observation cannot be generalized, because, with an increase in the size and number of opening, the stiffness of the beam could alter. Crack patterns of the beams are depicted in Fig. 8c. Overall crack pattern and failure mode were similar in all the three cases. In this case, the crack initiated from the periphery of the opening led to the failure of the beam. The failure of the beam occurred for all three cases due to the crack in the middle of the beam (Fig. 8c). Early collapse of the beam compared to the other two cases can be attributed to the opening located in the high moment area. A similar observation was reported by Mansur *et al.* (1991a) for beams with horizontal openings.

5. Finite element analysis

As seen from the previous sections, laboratory experiments were conducted with only three cases. The effect of vertical opening such as size and, the location

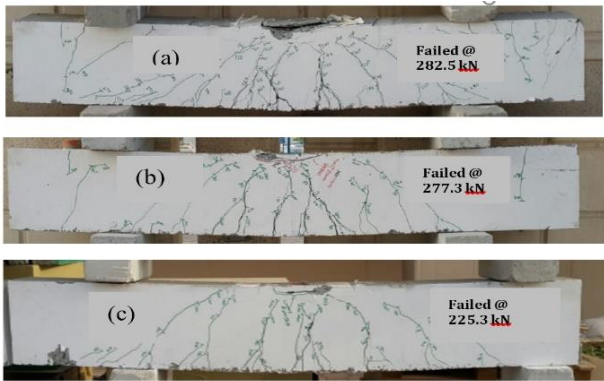


Fig. 8 crack patterns for the beams (a) beam without opening (b) 110 mm dia opening at 220 mm from the left edge of the beam (c) 110 mm dia opening in the middle of the beam

along the length and width of the beam are examined by numerical experiments using nonlinear finite element analysis (FEA). The FE model is benchmarked against the experimental results for two cases presented in the previous section. The benchmarked FE model is used for further numerical experiments with different diameter and locations. Constitutive material model of the reinforced concrete beam and reinforcements used for the numerical experiments are described in the subsequent sections.

5.1 Tensile behavior of concrete

A constitutive model for the total strain based on the modified compression field theory was originally proposed by Vecchio and Collins (1993). Three-dimensional extension to this theory proposed by Selby & Vecchio (1993) was employed in the present work. Discrete and smeared crack modeling approaches are in general employed for crack modeling in concrete. In the discrete approach, crack is modeled as a geometric discontinuity by disconnecting the cracked elements along its edges. On the other hand, a smeared crack model originally proposed by Rashid (1968) assumes the cracked solid to be a continuum. In the present study, the smeared crack model is employed. Linear tension cut off criterion was used for the crack initiation (DIANA, 2017). In other words, when the principal tensile stress exceeds the tensile strength of concrete, a new crack is developed. The coupling effects of different cracks are neglected and for an individual crack and all the crack stresses are solely governed by the corresponding crack. Softening relationship is expressed in terms of the fracture energy G_f^I through crack band width or element equivalent length h . In this investigation, linear tension softening was used as shown in Fig. 9. The reduced tensile strength is estimated using the expression given below;

$$f_t = \sqrt{2 \frac{G_f^I E_c}{h}} \quad (1)$$

In this study, the crack bandwidth is defined as, $h = \sqrt[3]{V}$, where V is the volume of the solid element. Cracked

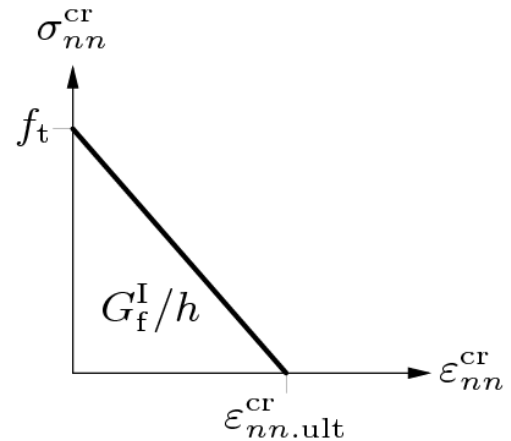


Fig. 9 Linear tension softening relationship for concrete

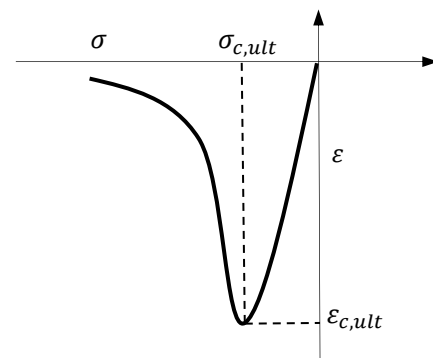


Fig. 10 Compression behavior of concrete

tensile strength is dependent on the element size h and material properties such as tensile strength and fracture energy.

5.2 Compression behavior of concrete

The stress-strain relationship of concrete in this study was modeled using Thorenfeldt (1987) curve as depicted in Fig. 10. The strength and ductility increase with the increase in isotropic stress and decrease with lateral cracking. These effects were incorporated while obtaining the failure function for compression. If the material was cracked in the lateral direction, the allowable peak stress and peak strain were reduced with a factor (DIANA 2017).

5.3 Reinforcement model

Reinforcement in concrete can be modeled either using the embedded concept or discrete modeling (DIANA, 2017). In the present study, main reinforcements and shear stirrups are modeled using embedded reinforcement. In the embedded reinforcement model, separate degrees of freedom or nodes are not added for reinforcement in the finite element model. However, the reinforcement is incorporated by contributing to the element stiffness and total beam stiffness matrix. Material behavior of the reinforcement is modeled using von-Mises plasticity (DIANA 2017).

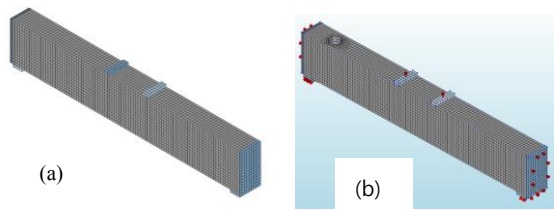


Fig. 11 Finite element mesh: (a) base line reinforced concrete beam without any opening (b) 110 mm dia opening in the beam at 220 mm from the left support.

Table 4 Comparison of FEA results with laboratory experiments

Sample Description	Laboratory experiment		Finite element analysis	
	Failure Load (kN)	Max Deformation (mm)	Failure load (kN)	% error
Reference beam without opening	282.5	20	279.7	1 %
110 mm dia opening @ 220 mm from the left support	277.3	17	272	2 %

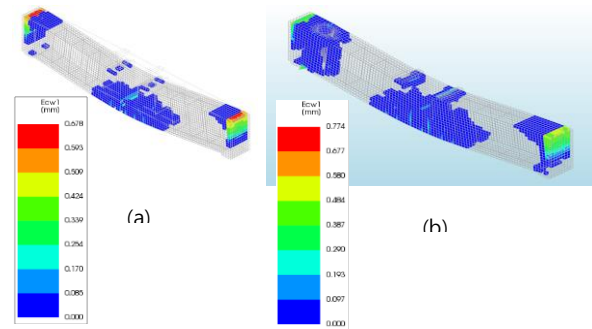
6. Results and discussion

6.1 Benchmarking of the finite element model

The finite element model was benchmarked using two laboratory experiments; beam without an opening and beam with an opening at 220 mm from the left end of the beam (Geometrical details of the beam are presented in Fig. 2). The RC beam was modeled using eight-nodded linear brick element (DIANA, 2017). The reinforcements (main bars and shear stirrups) were modeled using one dimensional embedded bar elements. As mentioned in the previous section, von-Mises plasticity is used to model the material behavior of the reinforcement bars. FE model for the beam without an opening and beam with an opening at 220 mm from the left end of the beam are shown in Figs 11a and 11b. Fixed support is incorporated in the FEA by constraining all translations XYZ directions (i.e., $U_x=U_y=U_z=0$).

The FE mesh size is an essential parameter in the nonlinear analysis as it depends upon the convergence and element crack definition. In this study, the beam was meshed using uniform element size of 5 mm x 5 mm based on the initial trial analysis. The fracture energy of 0.15 was used in the analysis. Compressive and tensile strengths of concrete were used as 39.56 MPa and 3.2 MPa respectively as obtained from the laboratory test.

FEA results are tabulated in Table 4, and the load-displacement curve is presented in Fig. 7. Average stiffness of the finite element model in the linear range is 30.95 kN/mm. Percentage error compared with the experimental result is 0.99%. For the reference beam without opening, the FEA predicted a failure load of 279.7 kN with 1% error with respect to the experimentally predicted failure load.



(a) Beam without opening (b) beam with an opening at 220 mm from the left support

Fig. 12 The crack pattern obtained from the FEA

Crack pattern and the principal crack width obtained from the FEA is presented in Fig. 12. As observed in the experimental case the first crack appeared in the soffit of the beam at the center. Cracked elements are shown highlighted in the Fig. 12. Major cracks are in the middle region and also near the fixed end of the beam as observed in the experiment. The crack patterns match quite well with the experimental observation. The failure of the beam was caused due to a vertical crack from the soffit of the middle section of the RC beam.

For the beam with an opening at 220 mm from the left support, the load-displacement curve and crack pattern are presented in Figs 7 & 12 respectively. Average stiffness of the finite element model in the linear range is 31.16 kN/mm. Percentage error compared with the experimental result of the beam with opening is 1.7%. It is interesting to note that the overall stiffness of the finite element model of beam with and without opening are almost same indicating that the opening did not alter the stiffness the beam. Similar observation was made in the laboratory tests results. The FEA predicted a failure load of 272 kN against the experimental value of 277.3 with 2% error. The FE model captured the load-displacement behavior, crack pattern and failure modes quite well. It is worth noting that the FE model showed relatively less ductility compared to the experimental values. The overall behavior (load-displacement relationship, failure load, and crack pattern) was predicted quite well by the finite element model. Hence the same model is used for further numerical experiments as described in the following section.

6.2 Numerical experiments using finite element analysis

6.2.1 Effect of a vertical opening with various position along the length

Numerical experiments are conducted using the benchmarked finite element model. In the first set of numerical analysis, the position of the center of the vertical opening, x , is moved along the length of the beam L . Here, x is the center of the opening from the left support of the beam, and L is the total length of the beam. The ratio of failure load of the beam with an opening at various location to the failure load of the beam without opening, P_f/P_{bf} is plotted against the ratio of the distance of the center of the opening from the left end of the beam to half length of the

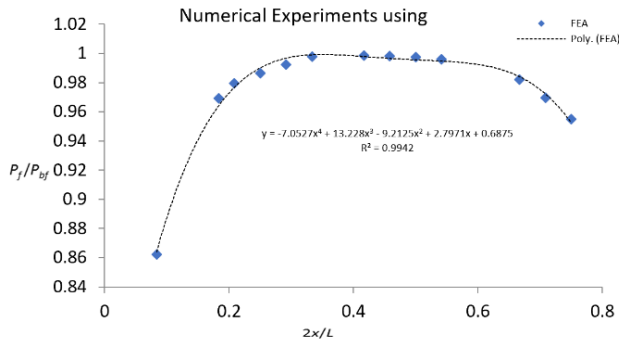


Fig. 13 Variation of failure load due to change in location of the opening along the length of the beam

beam, $2x/L$. Here, P_{bf} is failure load for the baseline case without opening obtained from the FEA, P_f is the failure load obtained from the FEA with an opening at different locations. 18 finite element simulations were carried out, and the results are plotted in Fig. 13. When the value of $2x/L$ is between 0.2 to 0.7, the failure load reduction is less than 3%. Hence, the optimum location of the opening is when the center of the opening is within this range (i.e., $2x/L$ is between 0.2 and 0.7). It is also worth mentioning that in this region the bending moment is low compared to the center of the beam. Finite element analysis results could not converge for the cases when the opening is near the center of the beam. Hence the finite element analysis results for these cases were not included in the plot. However, a least square error fit of the data was obtained from the available finite element data as shown in Fig. 13. The R^2 value of the least square error best-fit curve is 0.98. The order of the polynomial was chosen with respect to adjusted R^2 value. From the least square error fit, failure load when the center of the opening is in the middle of the beam is estimated with 20% reduction compared to the baseline finite element model. This prediction matches well with laboratory observations where the beam containing an opening in the middle of the beam failed at 19% lower load compared to the reference beam.

Similarly, 14% reduction in load carrying capacity is estimated when the opening is near the support where $2x/L = 0.09$. Such higher reduction in failure load is attributed to the higher bending moment near the support and in the center of the beam as reported earlier by Mansur *et al.* [24] for beams with horizontal openings. It is interesting to note that, for most practical purposes the beam openings are incorporated near the support (say at $2x/L < 0.1$). In such cases, the beam should be designed with 20% more load carrying capacity to account for the opening.

6.2.2 Effect of vertical opening due to various position along the width of the beam

In this section, variation of failure load due to different positioning along the y -axis is examined. For the purpose of the study, the location of the opening along the x -axis is chosen at 850 mm from the left support (i.e., $2x/L=0.708$). The center of the beam opening is moved along the Y -axis. Results of the analysis are presented in Fig. 14. The ratio of

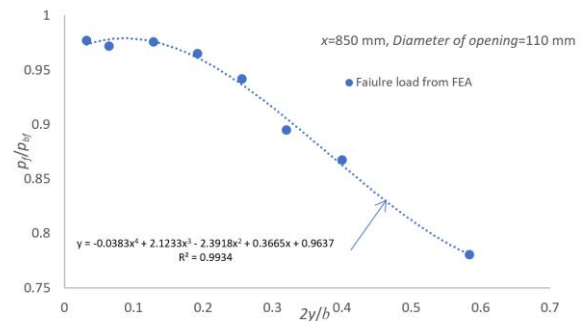


Fig. 14 Variation of failure load due to change in location of the opening along the width of the beam

the failure load for each Y -location with respect to the reference beam without opening is plotted against the ratio of location to the width of the beam, b . It is observed that, if the Y -position is displaced by a small amount (i.e., $y/b < 0.20$) from the center of the beam along the width, then, failure load is not altered much as seen in the graph. However, for $y/b > 0.2$, the slope of this curve is increased quite sharply indicating a drastic reduction in the failure load. In other words, the position tolerance of the beam opening along the y -axis (width of the beam) is quite small, especially for values of $y/b > 0.2$. Hence extra care should be taken while positioning the service pipe for the opening. When the center of the opening moved very close to the edge, so that the edge distance from the opening circumference is less than a threshold value (in this case, 30 mm), a sharp reduction in failure is observed. But in all practical cases, this may not occur, because, the service pipes are installed within the reinforcement cage. Hence, even if the pipe is misplaced, it will not go beyond the reinforcement cage.

6.2.3 Effect of size of the opening and edge distance

Effect of opening size on the failure load is examined here. In this exercise, the center of the opening is placed in the middle of the beam to maintain the geometric symmetry along the y -axis (at $x=850$ mm from the left support). Failure load ratio for various diameters is presented in Fig. 15. In this Fig., the ratio of d/b (X -axis,) is plotted against p_f/p_{bf} , where d is the diameter of the opening. It is clear from the graph that when d/b exceeds 0.25, there is a sharp change in the gradient of the curve and hence, sharp reduction in the estimated failure load. The sharp reduction is attributed to the limiting value of the combined effect of reduction in edge distance and reduction in the area of cross-section. To examine the effect of edge distance, reduction in failure load due to edge distance is plotted in Fig. 16. As seen in the previous graph, a sharp reduction in failure load is observed when the e/b ratio is reduced to less than 0.45 as indicated by the increased slope of the curve. Here e is the edge distance to the circumference of the opening, and the limiting value it is considered as the reinforcement cover. Further experimental work shall be carried out to examine this effect.

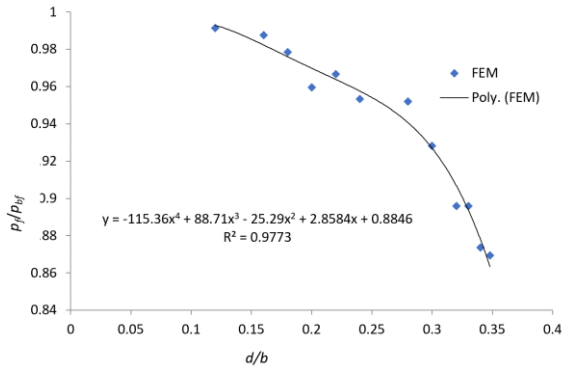


Fig. 15 Variation of failure load due to change diameter of the opening

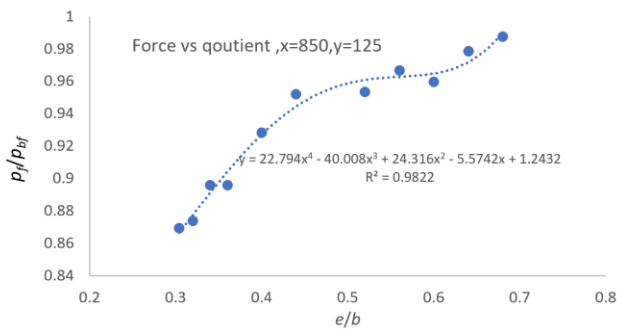


Fig. 16 Variation of failure load due to edge distance of the opening

7. Analysis using Artificial Neural Network (ANN)

To understand the complete effect of a vertical opening in an RC beam, the artificial neural network (ANN) analysis (Prasad *et al.*, (2009)) has been employed. Results from 50 finite element analyses (discussed in the previous sections) were used as input data in the ANN. The ANN analysis consisted of an input layer, hidden layer, and output layer. For each input variable, there are neurons in the input layers, and the input layer does not directly contribute to modeling the input-output relationship. The hidden layer performs the modeling part of the ANN and obtains the optimal relationship between the input and output. The accuracy of the ANN depends on the number of neurons in the hidden layer. Higher the number of neurons could improve the fit of the training set. It may also cause overfitting if a higher number of neurons were used in the model which could be detected in the in the test set. The values from the output layer are the final results of a neural network. Bayesian regularization algorithm was employed in the present study (Anctil *et al.*, (2004)). This algorithm is suitable for a small training set of data. In the present study, 30 datasets were used for the training, 10 datasets were used for validation, and the rest 10 sets were used for testing. In the present ANN model, variation in the position of opening along x and y , the diameter of the opening are used as the input variables. The low mean square error was obtained for all training validation and testing sets. The error histogram of the analysis is shown in Fig. 17. The errors are almost

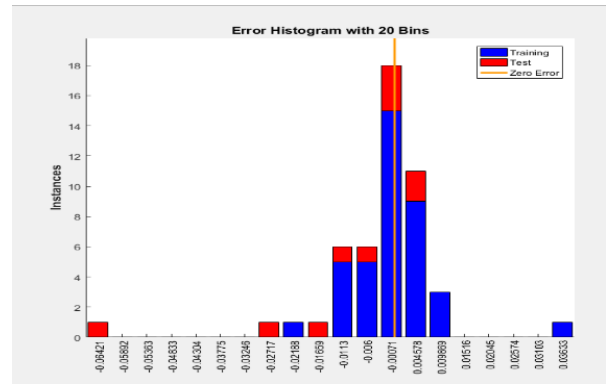


Fig. 17 Histogram for the ANN analysis

zero mean (unbiased) and appear to follow the normal distribution. The R^2 value of the result is 97.8%, which means that the model can account for most of the variability in the data.

ANN results are presented in Figs. 18 & 19. It is quite interesting to note that, when the opening is in the middle of the beam (i.e., $2x/L=1$) the load carrying capacity is reduced by 18%. ANN prediction is only 1% error with the experimentally observed value. When $2x/L$ is between 0.2 and 0.7, the reduction in load carrying capacity is minimal, and thus the optimum location for the beam opening is within this region. As mentioned earlier, this is also the region with relatively lower bending moment. When the beam opening is placed near the support (i.e., $2x/L=0.05$), the reduction in load carrying capacity is approximately 9%.

Fig. 19a shows the effect of a change in position of the center of the opening along the width (various values of $2y/b$). The result is a stepped curve indicating two limiting values for various values of $2y/b$. When $2y/b < 0.15$, the ratio, p_f/p_{fb} approaches 1 depending on the diameter of the opening, and x location along the length. The present curve is obtained with a diameter of the opening is 110 mm and with x location at 850 mm from the left support. For this case, the limiting value of p_f/p_{fb} will approach to 0.8. Similarly, when $2y/b > 0.2$, there is a sharp reduction in the ratio p_f/p_{fb} . When $2y/b = 0.3$, corresponds to an edge distance of 40 mm from the circumference of the opening. Hence, if the edge distance is less than 30 mm, a sharp decrease in p_f/p_{fb} is observed. Fig. 19b shows the effect of the diameter of the opening on p_f/p_{fb} . In this graph, the diameter of the opening is expressed in terms of the edge distance. As the edge distance decreases (with an increase of the diameter of the opening), the ratio p_f/p_{fb} reduces drastically.

8. Conclusion

In the present paper, RC beams with vertical openings are examined using laboratory experiments and non-linear FEA. Nine laboratory experiments and 50 nonlinear FE simulations are carried out. ANN analysis was carried out using the FEA generated data. FEA and ANN results are in good agreement with observations from the laboratory

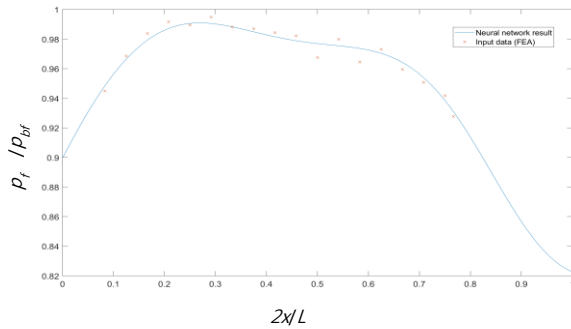


Fig. 18 Variation of failure load due to change in location of opening along the length of the beam using ANN

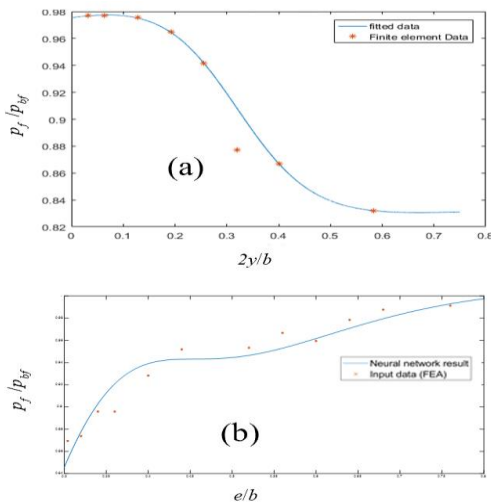


Fig. 19 Variation of failure load due to (a) diameter of the opening (b) edge distance of the opening using ANN

experiments. Various design parameters of the openings such as diameter and location along the length and width of the beam and edge distance are examined using numerical experiments. Following are the main observations from the current study.

1. Vertical opening placed near the center or support of a fixed-fixed beam reduces the load carrying capacity by around 20% compared to the beam without opening. These two regions have a high bending moment. The early collapse of the beam with an opening in these two regions is attributed the large moment values. Hence, as a general conclusion, beams containing vertical opening in the region of large bending moment could cause early collapse compared to a solid beam.

2. The stiffness of the beam, crack pattern, and failure modes are not affected due to a single vertical opening in the RC beam. This conclusion might not be able generalize for beams with multiple openings.

3. As the diameter of the vertical opening increases, the load carrying capacity reduces.

Variation of failure load with respect to the edge distance from the circumference of the opening along the width of the beam produced a step curve relationship. This indicates that the load carrying capacity is not altered until

the edge distance is reduced less than a threshold value (in this study, this value is attributed to the concrete cover). When the edge distance is less than this threshold value, failure load reduces drastically.

References

- Alvanitopoulos P.F., Andreadis I. and Elenas A. (2010), "Interdependence between damage indices and ground motion parameters based on Hilbert–Huang transform", *Measure. Sci. Technol.*, **21**(2), 025101-025115. <https://doi.org/10.1088/0957-0233/21/2/025101>.
- Chen, X., Nie, G.J., Jia, L.J. and Sun, B. (2013), "Approximate calculation of nature frequency of partially earth-anchored cable-stayed bridges", *Chinese Quarterly Mech.*, **34**(4), 650-655.
- Gimsing, N.J. and Georgakis, C.T. (2012), *Cable-Supported Bridges: Concept and Design*, John Wiley & Sons Ltd, Chichester, United Kingdom.
- Jin, Z.B., Pei, S.L., Wei, X., Liu, H. and Qiang, S. (2016), "Partially earth-anchored cable bridge: Ultra long-span system suitable for carbon-fiber-reinforced plastic cables", *J. Bridge Eng.*, **21**(6), [https://doi.org/10.1061/\(ASCE\)BE.1943-5592.0000877](https://doi.org/10.1061/(ASCE)BE.1943-5592.0000877).
- JTG D65-01 (2007), *Guidelines for design of Highway Cable-stayed Bridge*, Ministry of Communications, Beijing, China.
- JTG T B02-01 (2008), *Guidelines for Seismic Design of Highway Bridges*, Ministry of Communications, Beijing, China.
- Muller, J. (1991), "Bi-stayed Cable-stayed Bridge", *International Conference on Bridge*, 455-460. Leningrad, Russia.
- Shao, X.D., Hu, J. and Zhao, H. (2011), "Conceptual design of super-span cable-stayed bridge with partial ground-anchorage and cross stays", *J. Chongqing Jiatong U (Natural Sci.)*, **30**(S2), 1188-1191.
- Sun, B., Cheng, J. and Xiao, R.C. (2010), "Preliminary design and parametric study of a 1400 m partially earth-anchored cable-stayed bridge", *Sci. China Series E Technol. Sci.*, **53**(2), 502-511. <https://doi.org/10.1007/s11431-010-0041-4>.
- Sun, B., Xiao, R.C. and Cai, C.S. (2013), "Cost analysis of partially earth-anchored cable-stayed bridge", *J. Tongji U (Natural Sci.)*, **41**(10), 1476-1482.
- Sun, B., Cheng, J. and Xiao, R.C. (2015), "Optimization of dead load state in earth-anchored cable-stayed bridges", *J. Harbin Institute Technol.*, **22**(3), 87-94.
- Won, J.H., Park, S.J., Yoon, J.H. and Kim, S. (2008a), "Structural effects of partially earth-anchored cable system on medium span cable-stayed bridges", *J. Steel Struct.*, **8**(3), 225-236.
- Won, J.H., Yoon, J.H., Park, S.J. and Kim, S. (2008b), "Effects of partially earth-anchored cable system on dynamic wind response of cable-stayed bridges", *Wind Struct.*, **11**(6), 441-453. <https://doi.org/10.12989/was.2008.11.6.441>.
- Xiang, H.F. (2012), "The trend of the world's mega-scale bridges—An inspiration of IABSE 2011 in London", *Bridge*, **3**, 12-16.
- Xiao, R.C. (2013), *Bridge Structural Systems*, China Communications Press, Beijing, 166-174.
- Xiao, R.C., Wei, P. and Sun, B. (2013), "Mechanical analysis and parametric study of long-span partially earth-anchored cable-stayed bridge", *J. Southeast U (Natural Sci.)*, **43**(5), 1097-1103.
- Zhang, L.W., Xiao, R.C. and Xia, R.J. (2011), "Mechanical analysis and study on structural parameter of partially earth-anchored cable-stayed bridge part I: Mechanical analysis", *Appl. Mech. Mater.*, **44**, 1898-1905. <https://doi.org/10.4028/www.scientific.net/AMM.44-47.1898>.
- Zhang, X.J. and Yao, M. (2015), "Numerical investigation on the wind stability of super long-span partially earth-anchored cable-stayed bridges", *Wind Struct.*, **21**(4), 407-424. <https://doi.org/10.12989/was.2015.21.4.407>.

Zhang, X.J. and Yu, Z.J. (2015), "Study of seismic performance of cable-stayed-suspension hybrid bridges", *Struct. Eng. Mech.*, **55**(6), 1203-1221. <https://doi.org/10.12989/sem.2015.55.6.1203>.

CC